

Corneal Protein Nitration in Experimental Uveitis

MUTAY ASLAN,^{*}1 İCLAL YUCEL,[†] AKIF CİFTCIOĞLU,[‡] BERNA SAVAŞ,[§] YUSUF AKAR,[†]
GULTEKİN YUCEL,^{*} AND SALİH SANLIOĞLU^{||}

Departments of ^{}Biochemistry, [†]Ophthalmology, and [‡]Pathology, Akdeniz University School of Medicine, Antalya 07070, Turkey; [§]Department of Pathology, Ankara University Medical School, Ankara 06100, Turkey; and ^{||}Human Gene Therapy Unit, Akdeniz University School of Medicine, Antalya 07070, Turkey*

Increased expression of inducible nitric oxide synthase (NOS-2) in inflammatory diseases like uveitis suggests that it contributes to the observed pathological state. The aim of this study was to evaluate corneal expression of NOS-2 and corneal protein nitration in a rat model of uveitis. A single injection of intravitreal lipopolysaccharide was used to induce uveitis. Corneal proteins were separated by sodium dodecyl sulfate-polyacrylamide gel electrophoresis and visualized by Coomassie blue staining. Expression of NOS-2 and nitrotyrosine (NO₂Tyr) formation were determined *via* immunohistochemistry and Western blot analysis. Total nitrate/nitrite levels in the vitreous were measured by spectral analysis *via* the Griess reagent. Immunohistochemical analysis revealed increased corneal NOS-2 and NO₂Tyr immunoreactivity in rats with uveitis compared with controls. NOS-2 and NO₂Tyr immunoreactivity was observed in and around basal cells in the corneal epithelium. Western blot analysis of corneal lysates showed multiple nitrated protein bands in uveitic rats. Spectrophotometric measurement of total nitrate/nitrite levels in the vitreous affirmed significantly increased levels of nitric oxide generation in uveitis ($126 \pm 2.63 \mu\text{M}/\text{mg}$ protein) compared with controls ($65 \pm 6.57 \mu\text{M}/\text{mg}$ protein). The presented data suggests that extensive formation of protein nitration and reactive nitrogen species in the cornea contributes to tissue destruction in uveitis. Hence, selective inhibition of NOS-2 may prevent long-term complications and lead to an improvement in the management of uveitis. *Exp Biol Med* 232:1308–1313, 2007

Key words: uveitis; cornea; nitration; inducible nitric oxide synthase

This study was supported by a grant from Akdeniz University Research Foundation, Turkey (2003.01.0103.007).

¹ To whom correspondence should be addressed at Akdeniz University Medical School, Department of Biochemistry, 07070 Antalya, Turkey. E-mail: mutayaaslan@akdeniz.edu.tr

Received February 16, 2007.
Accepted July 9, 2007.

DOI: 10.3181/0702-RM-34
1535-3702/07/23210-1308\$15.00
Copyright © 2007 by the Society for Experimental Biology and Medicine

Introduction

Intraocular inflammation, most often called uveitis, is a major cause of severe visual impairment (1). Uveitis can lead to destruction of intraocular tissues by causing edema and high intraocular pressure (2). Multiple sclerosis, idiopathic optic neuritis, autoimmune corneal endotheliopathy, sarcoidosis, thyroid diseases, and inflammatory bowel diseases have all been associated with uveitis (3). Endotoxin-induced uveitis (EIU) has been widely used as an experimental model of uveitis (4, 5). Leukocyte adhesion, retinal cell injury, and apoptosis have all been reported in the eye after injection of a single dose of sublethal bacterial lipopolysaccharide (LPS) (6).

Nitric oxide (NO) is synthesized by a family of NO synthase (NOS) enzymes. Physiological amounts of NO synthesized by endothelial NOS (eNOS or NOS-3) and neuronal NOS (nNOS or NOS-1) participate in neurotransmission and vascular signaling, whereas accelerated NO production by inducible NOS (iNOS or NOS-2) results in cytotoxicity (7). Previous studies in uveitic rats have reported the presence of NOS-2 immunoreactivity in vitreal inflammatory cells, the iris, the ciliary body, and inner retinal layers (5, 8). Similarly, intravitreal injection of LPS into rabbits resulted in NOS-2 expression in corneal fibroblasts and corneal epithelium (9). Accelerated NO production by NOS-2 results in cytotoxicity *via* direct reactions of NO and the formation of secondary species capable of oxidation and nitration reactions. Indeed, reduction of corneal edema is seen in uveitic rats after application of N^G-nitro-L-arginine methyl ester, an NOS inhibitor (10).

The oxidation and nitration of lipids, amino acids, and proteins will alter biomolecular structure and function and at the same time reveal the pathogenic actions of reactive species (11). Corneal protein nitration has been observed in human corneal diseases such as keratoconus, Fuchs endothelial dystrophy, and in stored human corneal epithelium (12). Photoablated rabbit corneas have also

revealed extensive protein nitration (9). This study aimed to examine corneal protein nitration in a rat model of EIU, which has not previously been investigated. Expression of NOS-2 and formation of NO was also studied in all experimental groups reported herein.

Materials and Methods

Rat Model of Ocular Inflammation. All experimental protocols conducted on rats were performed in accordance with the standards established by the Institutional Animal Care and Use Committee at Akdeniz University Medical School. Male Wistar rats (obtained from Experimental Laboratory Animals Unit, Akdeniz University Faculty of Medicine) weighing 350–450 g were housed in stainless steel cages and given food and water *ad libitum*. Animals were maintained at 12:12-h light:dark cycle and a constant temperature of $23^{\circ} \pm 1^{\circ}\text{C}$ at all times. Twelve male Wistar rats were included in the study. Rats were divided into two groups of six animals each: Group 1, control; Group 2, LPS treated.

Ocular inflammation was induced *via* a single injection of intravitreal LPS as previously described (5). Briefly, LPS from *Salmonella typhimurium* (Sigma-Aldrich Chemie, Steinheim, Germany) was dissolved in sterile phosphate-buffered saline (PBS) at a concentration of 1 mg/ml. Rats were anesthetized intraperitoneally with a mixture of ketamine (25 mg/kg; Richter Pharma AG, Wels, Austria) and xylazine hydrochloride (5 mg/kg; Alfasan International B.V., Woerden, Holland), and 5 μg of LPS was injected into the vitreous of each eye. The controls received intravitreal injections of LPS-free PBS. Pain relief was provided to all rats *via* intramuscular (im) injections of tramadol hydrochloride (2 mg/kg; CONTRAMAL, Abdi Ibrahim, Istanbul, Turkey), given twice with 12-hr intervals, following intravitreal injections. Enucleation was performed 24 hrs after LPS injection in all experimental groups.

Immunohistochemical Staining. Enucleated globe materials were fixed in 10% buffered formalin solutions and incised in transverse plane just from the center of the globe to obtain two equal parts. Fixed tissues were washed in PBS (pH 7.4), embedded in paraffin, and cut into 4- μm sections. For peroxidase staining, sections were deparaffined, rehydrated, and washed with Tris-buffered saline. Endogenous peroxidase activity was blocked by incubating tissue sections with 3% hydrogen peroxide for 5 mins prior to application of the primary antibody. Primary antibody incubations were at 25°C for 60 mins using rabbit polyclonal anti-NOS2 (1:100 dilution; Santa Cruz Biotechnology, Santa Cruz, CA) and anti-nitrotyrosine (anti-NO₂Tyr; 10 $\mu\text{g}/\text{ml}$; Cayman Chemical, Ann Arbor, MI). After sections were washed they were immunostained with an avidin-biotin complex kit (Dako, Carpinteria, CA) followed by hematoxylin counterstaining. To assess non-specific staining for anti-NO₂Tyr, control experiments were performed by preadsorbing anti-NO₂Tyr with 10 mM

NO₂Tyr. Negative controls were also performed by replacing the primary antibody with nonimmune serum followed by immunoperoxidase staining. Presence of a red-brown-colored end product in the cytoplasm was indicative of positive staining. Counterstaining with hematoxylin resulted in a pale to dark blue coloration of cell nuclei.

To obtain a quantitative standard for polymorphonuclear cell infiltration within the different experimental groups, morphometric analysis was performed on all corneal sections by a pathologist blinded to the experimental conditions.

Sodium Dodecyl Sulfate-Polyacrylamide Gel Electrophoresis (SDS-PAGE) and Western Blot Analysis. Cornea was harvested from enucleated globes and homogenized in 2 ml ice-cold homogenizing buffer (50 mM K₂HPO₄, 80 μM leupeptin (Sigma-Aldrich, Steinheim, Germany), 2.1 mM Pefabloc SC (SERVA, Heidelberg, Germany), 1 mM phenylmethylsulfonyl fluoride (Sigma-Aldrich), 1 $\mu\text{g}/\text{ml}$ aprotinin (SERVA; pH 7.4). Homogenates were centrifuged (40,000 g, 30 mins, 4°C) and supernatants were stored at -80°C until analyzed. For Western blot analysis, tissue proteins were separated by SDS-PAGE and transferred to nitrocellulose membranes. A rabbit polyclonal antibody against anti-NO₂Tyr (5 $\mu\text{g}/\text{ml}$; Cayman Chemical) and anti-NOS-2 (1:800 dilution; BD Transduction Laboratories, San Jose, CA) were used for immunoblot analysis. Horseradish peroxidase-conjugated goat anti-rabbit IgG (1:10,000 dilution; Zymed Laboratories, San Francisco, CA) was used as a secondary antibody, and immunoreactive proteins were visualized by chemiluminescence *via* ECL reagent (Amersham Pharmacia Biotech, Buckinghamshire, England). Proteins separated by SDS-PAGE were also visualized by Electro-Blue Staining solution (Qbiogene, Heidelberg, Germany).

Nitrite and Nitrate Assay. Samples were transferred to an ultrafiltration unit and centrifuged through a 10-kDa molecular mass cut-off filter (Amicon, Millipore Corporation, Bedford, MA) for 1 hr to remove protein. Analyses were performed in duplicate *via* the Greiss reaction using a colorimetric assay kit (Calbiochem, Darmstadt, Germany). Protein concentrations were measured at 595 nm by a modified Bradford assay using Coomassie Plus reagent with bovine serum albumin as a standard (Pierce Chemical Company, Rockford, IL).

Results

Histological Analysis. Figure 1 illustrates photomicrographs of corneal cross sections from representative rats of each of the two experimental groups. Apparent differences were observed in the histological evaluation of the cornea. When compared to the control group, LPS-treated rats displayed extensive polymorphonuclear (PMN) cell infiltration accompanied by stromal edema. Light microscopic observations of inflammation were confirmed by morphometric analysis which quantified PMN cell

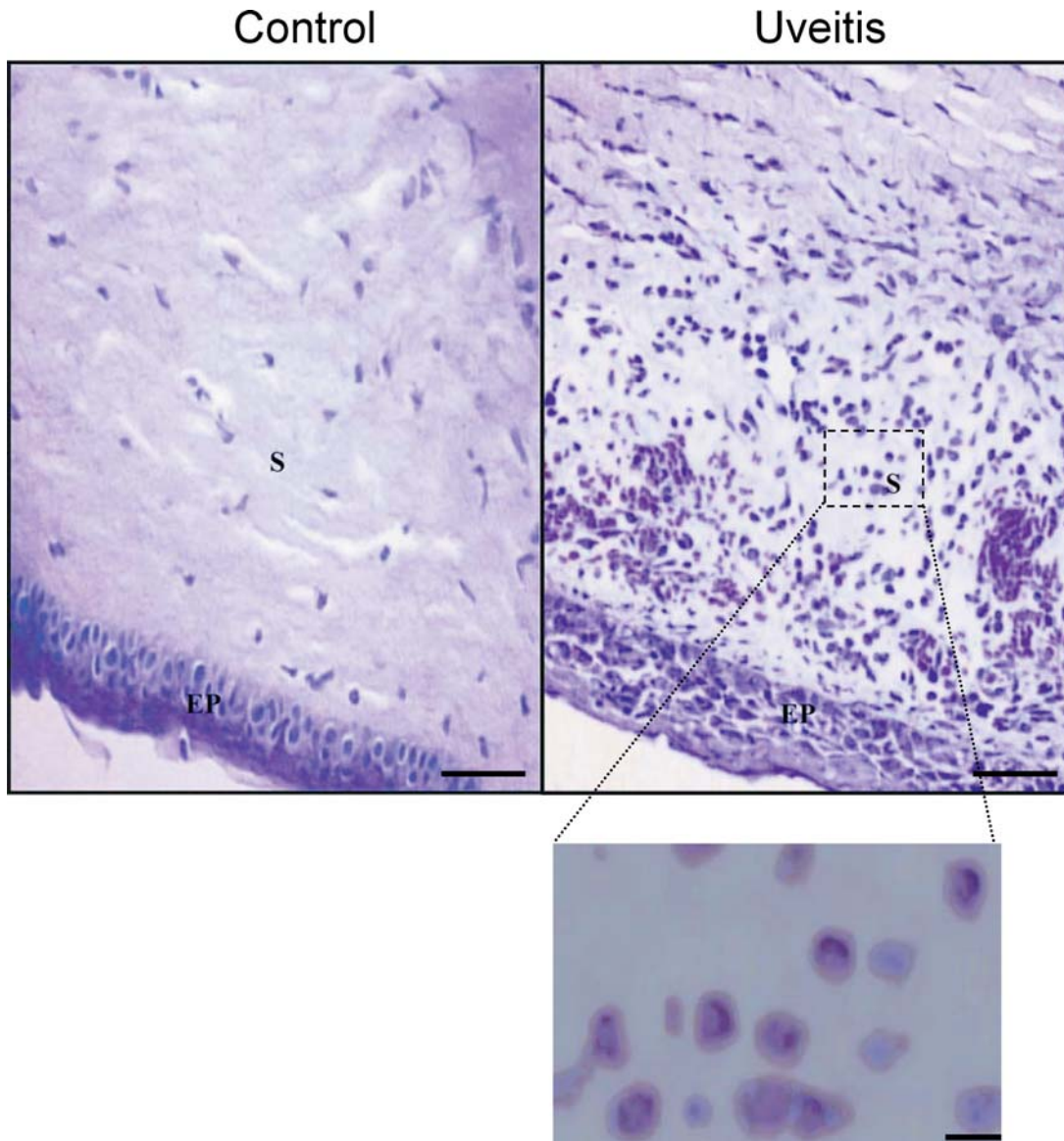


Figure 1. Hematoxylin and eosin staining of the rat cornea. Corneal photomicrographs of a representative rat are shown from control and uveitis groups. EP, corneal epithelium; S, stroma. Bars, 50 μ m. Higher-magnification corneal image of the LPS-injected eye is inserted below as indicated. Bar, 10 μ m. Color figure is available in the online version of the journal.

numbers in both the control and LPS-treated groups. As shown in Table 1, the number of cells/high power field (mean \pm SEM) ($n = 6$) was significantly increased in rats treated with LPS ($P = 0.002$).

NOS-2 Expression. LPS treatment caused a signifi-

Table 1. Number of Polymorphonuclear Cells in the Cornea

Group	PMN/HPF ^a
Control	5.1 \pm 2.36
Uveitis	60.6 \pm 13*

^a PMN/HPF, polymorphonuclear cells/high-power field ($\times 400$).

* $P = 0.002$, significant difference from control.

cant increase in NOS-2 protein expression, as determined by both Western blot analysis ($n = 3$) and immunohistochemical staining ($n = 6$). Figure 2A demonstrates the localization of NOS-2 in corneal cross sections in each of the two experimental groups. NOS-2-positive staining was observed in and around basal cells in the corneal epithelium. NOS-2 was not present in the cornea of control rats. Western blot analysis of corneal homogenates using an anti-NOS2 antibody also revealed a 130-kDa protein band present only in diseased rat groups (Fig. 2B).

NO₂Tyr Formation. The localization of protein NO₂Tyr in corneal cross sections is demonstrated in Figure 3A. NO₂Tyr-positive staining was observed in and around basal cells in the corneal epithelium. Protein nitration was

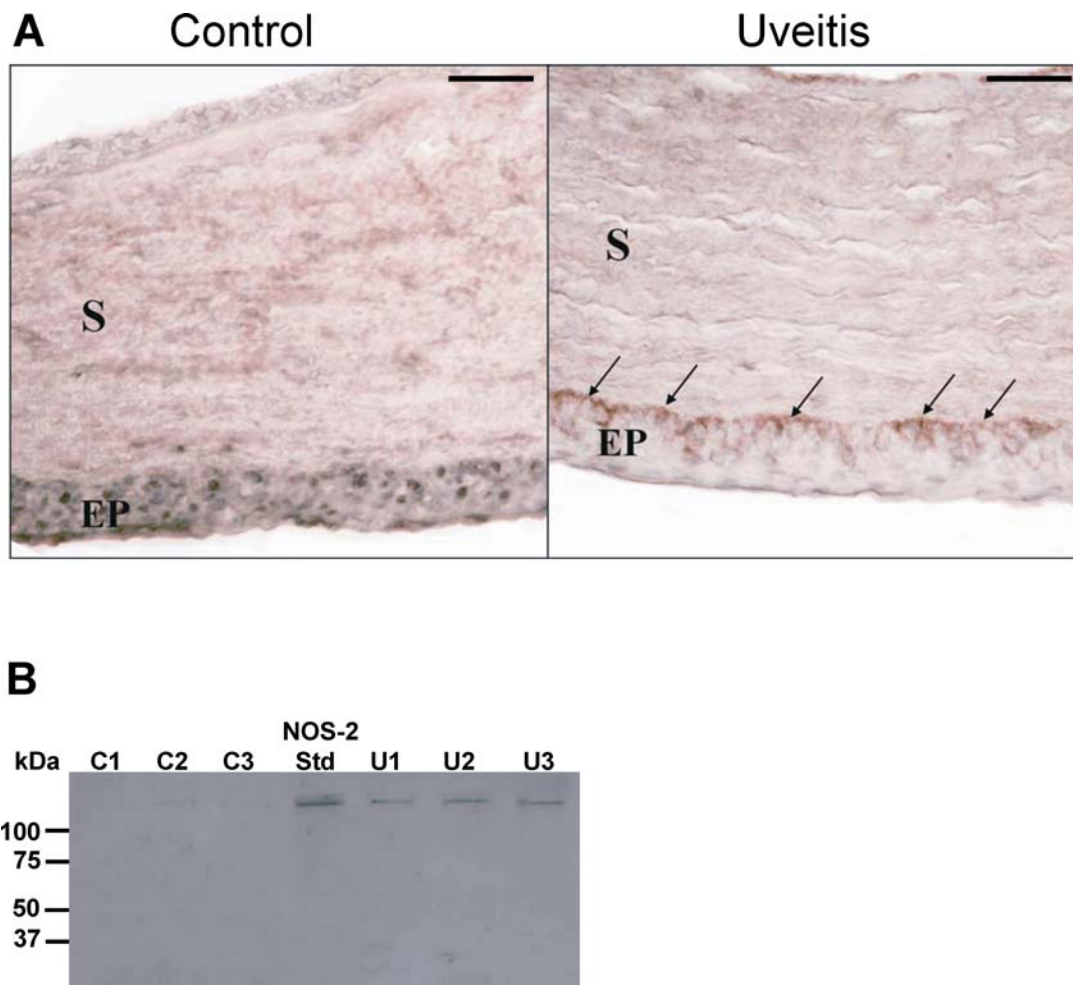


Figure 2. (A) Immunostaining of NOS-2 in the cornea. Corneal photomicrographs of a representative rat are shown from control and uveitis groups. EP, corneal epithelium; S, stroma. Bars, 30 μ m. (B) Western blot analysis of corneal homogenates analyzed by immunoblotting with rabbit polyclonal antibody against NOS-2. For each sample, 50 ng of NOS-2 standard and 45 μ g of total tissue protein was loaded. C, control; U, uveitis. Color figure is available in the online version of the journal.

present only in diseased rats and not in the controls. Corneal homogenates from all experimental groups were also analyzed by SDS-PAGE and visualized by both Western blot analysis using anti-NO₂Tyr antibody and Coomassie blue staining for proteins. Western blot analysis of corneal homogenates using an anti-NO₂Tyr antibody revealed multiple immunoreactive protein bands with molecular weights of 50 kDa or less (Fig. 3B). Comparison of the immunoreactivity pattern seen in the Western blots with protein staining showed that retinal proteins were not equally nitrated (Fig. 3C).

Nitrite and Nitrate Concentration. Spectrophotometric measurement of total nitrate/nitrite levels in the vitreous affirmed significantly increased levels of nitric oxide generation in LPS-treated rats ($126 \pm 2.63 \mu$ M/mg protein) compared with controls ($65 \pm 6.57 \mu$ M/mg protein). Values are mean \pm SEM ($n = 5-6$). The statistical analysis of the obtained data was performed by Sigma Stat (version 2.03; Systat Software Inc., San Jose, CA) software for windows. The differences among the different groups were

analyzed *via* the Student's *t* test, with significance at $P < 0.01$ versus control.

Discussion

It is reported herein that increased corneal NOS-2 expression and excessive NO formation lead to corneal protein nitration in experimental uveitis. To our knowledge this is the first study to report corneal protein nitration in experimental uveitis.

EIU can be created by injecting a single sublethal dose of bacterial LPS into the footpad or vitreus of an experimental animal. When LPS is injected into the footpad, uveitis occurs in both eyes, and the severity of inflammation can vary from animal to animal. Intravitreal injection of LPS increases reproducibility and causes a similar degree of ocular inflammation in all injected animals. Reported studies have documented that this method of EIU causes severe fibrinoid exudation in the papillary area, with intense flare in the anterior chamber at 24 hrs after injection (5). These symptoms compare to grade 4 (full score) uveitis

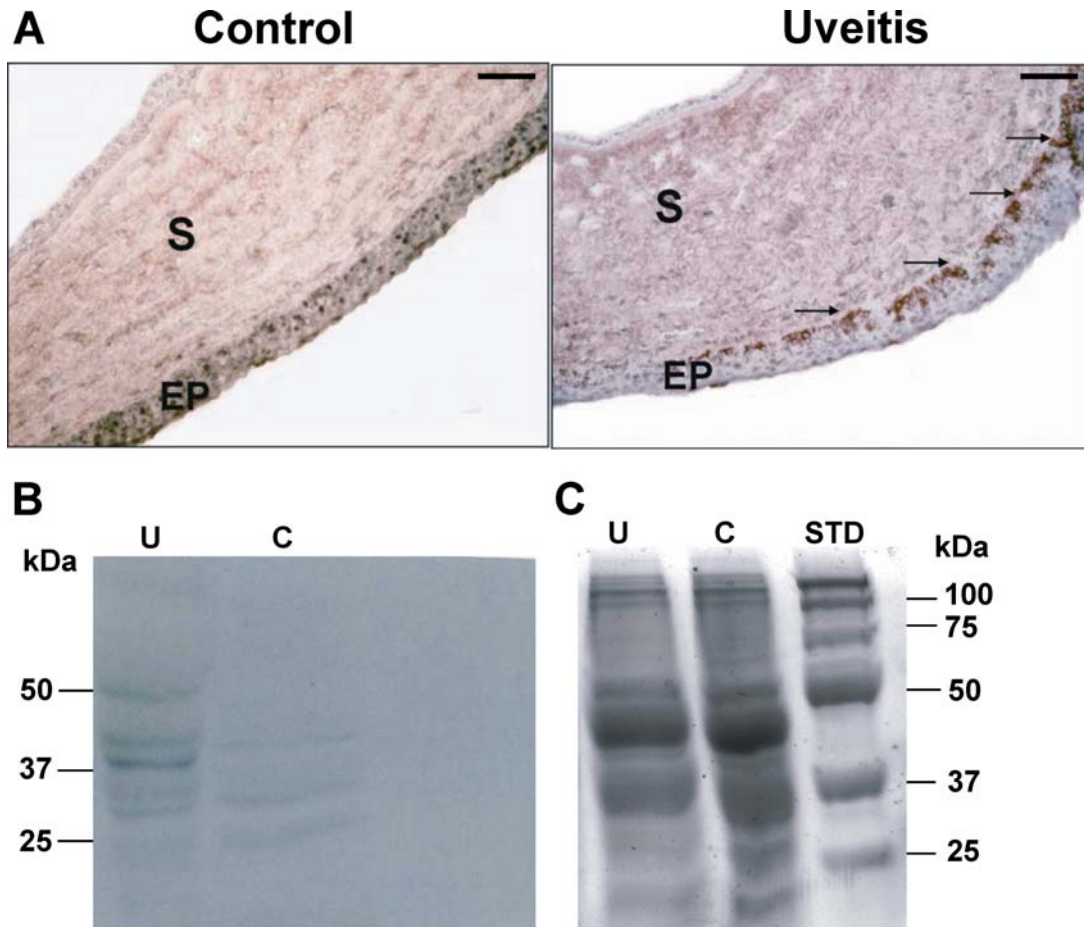


Figure 3. (A) Immunostaining of 3-nitrotyrosine in the cornea. Corneal photomicrographs of representative rat are shown from control and uveitis groups. EP, corneal epithelium; S, stroma. Bars, 30 μ m. (B) Western blot analysis of corneal homogenates analyzed by immunoblotting with rabbit polyclonal antibody against 3-nitrotyrosine. (C) SDS-PAGE analysis of corneal homogenates. Corneal proteins were separated by SDS-PAGE and visualized by Coomassie blue staining. STD, molecular weight standards; C: control; U: uveitis. Color figure is available in the online version of the journal.

(13); therefore, enucleation was performed 24 hrs after LPS injection.

Although uveitis is reported to involve mainly the anterior uvea and inner layers of the retina, the involvement of the cornea has also been suggested (10). As shown in Figure 1, extensive corneal PMN cell infiltration in uveitic rats was accompanied by stromal edema. This observation is in agreement with previous studies that report corneal ultrastructural pathology during EIU. Alterations in corneal endothelial and epithelial cells and corneal edema have been demonstrated during uveitis (10).

Corneal NOS-2 expression has been previously observed in rabbits treated with intravitreal LPS (9). In the reported study, NOS-2 was expressed in many inflammatory cells and fibroblasts in the corneal stroma. In this study, NOS-2-positive staining was mainly observed in and around basal cells in the corneal epithelium (Fig. 2). This observation is in accord with human studies that have identified NOS-2 staining in the epithelium of diseased corneas obtained from patients with bullous keratopathy, Fuchs dystrophy, and keratoconus corneas (12). The

presence of NOS-2 in diseased corneas could be linked to the production of inflammatory cytokines that induce the expression of NOS-2. The cornea can be exposed to these cytokines either *via* the infiltrating PMN cells or by activated corneal cells (10). Indeed, tumor necrosis factor- α , which promotes NOS-2, is expressed in the cornea during the initial phase of inflammation (4). Similarly, interleukin-1 β mRNA is induced in the cornea at a similar time course as that seen in the iris-ciliary body (14).

As seen in Figures 2 and 3A, the staining pattern for NOS-2 and NO₂Tyr appear to correlate. That is to say, areas expressing NOS-2 corresponded to areas staining for NO₂Tyr. Protein nitration observed during uveitis could be either *via* the formation of the oxidizing and nitrating species peroxynitrite (ONOO⁻) (15) or by peroxidase-catalyzed oxidation of nitrite (NO₂⁻), an NO metabolite that is elevated in uveitis to the nitrating species nitrogen dioxide (NO₂) (16). Myeloperoxidase (MPO), a heme peroxidase released during neutrophil, monocyte, and macrophage activation, can give rise to nitrotyrosine formation (11). As stated previously, LPS-induced changes in corneal cell

ultrastructure initiate an inflammatory response which is causally linked to activation and adherence of neutrophils. It is well known that when neutrophils are activated by a proinflammatory signal the granules fuse with the plasma membrane in a simultaneous manner and discharge their contents into the extracellular medium (17). This process, also called degranulation, is a way by which MPO is released into sites of inflammation. The potential of MPO to diffuse away from areas of direct neutrophil infiltration and cause protein nitration was demonstrated using immunohistochemical techniques that illustrated the colocalization of MPO with areas of NO₂Tyr formation (18).

NO₂Tyr-positive staining observed in and around basal cells in the epithelium can lead to altered protein function within the cornea. A major function of corneal epithelium is to serve as a permeability barrier against the accumulation of fluid from the tear (19). In fact, studies have confirmed the existence of an NaK-ATPase (20) pump and an active Cl transport system (21) in the corneal epithelium that result in a net transfer of Na and Cl from the stroma to tears in the presence of a resting potential (22). Altered epithelial NaK-ATPase and Na-Cl pump activities can thus play a role in corneal edema observed in uveitis. *In vitro* reaction of 100–500 μM ONOO⁻ with purified Na₂K-ATPase has been shown to nitrate the 110-kDa alpha-3 catalytic and 50-kDa beta transport subunits, as quantified by immunoblots of the reaction products for NO₂Tyr (22). Western blot analysis of corneal homogenates from uveitic rats using an anti-NO₂Tyr antibody revealed an immunoreactive protein band with a molecular weight of 50 kDa (Fig. 3B) that may be speculated to function as a protein involved in epithelial ion transport.

In summary, immunohistochemical staining and Western blot analysis of the cornea revealed increased NOS-2 and nitrated protein immunoreactivity in uveitis. The presented data suggests that extensive formation of protein nitration in the cornea contributes to tissue destruction in uveitis. Hence, selective inhibition of NOS-2 may prevent long-term corneal complications and lead to an improvement in the management of uveitis.

- Durrani OM, Meads CA, Murray PI. Uveitis: a potentially blinding disease. *Ophthalmologica* 218:223–236, 2004.
- Kuchtey RW, Lowder CY, Smith SD. Glaucoma in patients with ocular inflammatory disease. *Ophthalmol Clin North Am* 18:421–430, 2005.
- Bonfioli AA, Damico FM, Curi AL, Orefice F. Intermediate uveitis. *Semin Ophthalmol* 20:147–154, 2005.
- Koizumi K, Poulaki V, Doehmen S, Welsandt G, Radetzky S, Lappas A, Kociok N, Kirchof B, Jousen AM. Contribution of TNF-alpha to leukocyte adhesion, vascular leakage, and apoptotic cell death in endotoxin-induced uveitis in vivo. *Invest Ophthalmol Vis Sci* 44:2184–2191, 2003.
- Koga T, Koshiyama Y, Gotoh T, Yonemura N, Hirata A, Tanihara H, Negi A, Mori M. Coinduction of nitric oxide synthase and arginine metabolic enzymes in endotoxin-induced uveitis rats. *Exp Eye Res* 75: 659–667, 2002.
- Aslan M, Yucel I, Akar Y, Yucel G, Ciftcioglu MA, Sanlioglu S. Nitrotyrosine formation and apoptosis in rat models of ocular injury. *Free Radic Res* 40:147–153, 2006.
- Alderton WK, Cooper CE, Knowles RG. Nitric oxide synthases: structure, function and inhibition. *Biochem J* 57:593–615, 2001.
- Yucel I, Akar Y, Yucel G, Ciftcioglu MA, Keles N, Aslan M. Effect of hypercholesterolemia on inducible nitric oxide synthase expression in a rat model of elevated intraocular pressure. *Vision Res* 45:1107–1114, 2005.
- Kim JC, Park GS, Kim JK, Kim YM. The role of nitric oxide in ocular surface cells. *J Korean Med Sci* 17:389–394, 2002.
- Behar-Cohen FF, Savoldelli M, Parel JM, Goureau O, Thillaye-Goldenberg B, Courtois Y, Pouliquen Y, de Kozak Y. Reduction of corneal edema in endotoxin-induced uveitis after application of L-NAME as nitric oxide synthase inhibitor in rats by iontophoresis. *Invest Ophthalmol Vis Sci* 39:897–904, 1998.
- Baker L, Freeman BA, Aslan M. Protein targets and functional consequences of tyrosine nitration in vascular disease. In: Dalle-Donne I, Scaloni A, Butterfield A, Eds. *Redox Proteomics: From protein modifications to cellular dysfunction and diseases*. Hoboken, NJ: John Wiley & Sons, Inc, pp729–786, 2006.
- Buddi R, Lin B, Atilano SR, Zorapapel NC, Kenney MC, Brown DJ. Evidence of oxidative stress in human corneal diseases. *J Histochem Cytochem* 50:341–351, 2002.
- Ruiz-Moreno JM, Thillaye B, de Kozak Y. Retino-choroidal changes in endotoxin-induced uveitis in the rat. *Ophthalmic Res* 24:162–168, 1992.
- Planck SR, Huang XN, Robertson JE, Rosenbaum JT. Cytokine mRNA levels in rat ocular tissues after systemic endotoxin treatment. *Invest Ophthalmol Vis Sci* 35:924–930, 1994.
- Beckman JS, Beckman TW, Chen J, Marshall PA, Freeman BA. Apparent hydroxyl radical production by peroxynitrite: implications for endothelial injury from nitric oxide and superoxide. *Proc Natl Acad Sci U S A* 87:1620–1624, 1990.
- Eiserich JP, Hristova M, Cross CE, Jones AD, Freeman BA, Halliwell B, van der Vliet A. Formation of nitric oxide-derived inflammatory oxidants by myeloperoxidase in neutrophils. *Nature* 391:393–397, 1998.
- Weiss SJ. Tissue destruction by neutrophils. *N Engl J Med* 320:365–376, 1989.
- Baldus S, Eiserich JP, Brennan ML, Jackson RM, Alexander CB, Freeman BA. Spatial mapping of pulmonary and vascular nitrotyrosine reveals the pivotal role of myeloperoxidase as a catalyst for tyrosine nitration in inflammatory diseases. *Free Radic Biol Med* 33:1010–1012, 2002.
- Edelhauser HF. The balance between corneal transparency and edema: the Proctor Lecture. *Invest Ophthalmol Vis Sci* 47:1754–1767, 2006.
- Ruf W, Ebel H. (Na+K+)-activated ATPase in human cornea. Distribution within the cornea and properties of the enzyme from epithelial cells. *Pflugers Arch* 366:203–210, 1976.
- SD Klyce. Transport of Na, Cl, and water by the rabbit corneal epithelium at resting potential. *Am J Physiol* 228:1446–1452, 1975.
- Golden WC, Brambrink AM, Traystman RJ, Shaffner DH, Martin LJ. Nitration of the striatal Na,K-ATPase alpha3 isoform occurs in normal brain development but is not increased during hypoxia-ischemia in newborn piglets. *Neurochem Res* 28:1883–1889, 2003.